Time Delayed SMC for Structural Stabilization of Chaotic Systems

Baghdadi HAMIDOUCHE[1], Kamel GUESMI[2], Najib ESSOUNBOULI[2]

[1]LAADI, FST, University of Djelfa (Algeria)

[2]Université de Reims Champagne-Ardenne, CReSTIC, France

E-mail: b.hamidouche@univ-djelfa.dz

Abstract - The objective of this paper is to achieve robust control and stability of chaotic systems by integrating sliding-mode control with time-delay techniques. This approach aims to stabilize the system's unstable periodic orbits (UPOs). We seek to ensure both the convergence of the sliding surface to zero and the minimization of the error between the system's current state and the delayed state corresponding to the UPOs. To identify the UPOs, we utilize the Poincaré map. The Lyapunov stability theory is then applied to validate the effectiveness of the proposed method. Through numerical experiments, this study showcases the ease of implementation, stability, effectiveness, and robustness of the method**.**

Keywords - Chaotic systems, Sliding mode control, Time-delayed system, Unstable periodic orbits, Rossler system.

I. INTRODUCTION

Sliding Mode Control (SMC) stands out in engineering for its exceptional ability to maintain stability in the face of various uncertainties and disturbances, solidifying its position as a powerful nonlinear control strategy. Pioneered in the 1970s by Emelyanov, Utkin, and Itkis [1], SMC boasts remarkable versatility, finding applications across diverse fields like engineering [2], robotics [3], aerospace [4], and control theory [5]. Its adept handling of nonlinear system control and stabilization makes SMC a valuable tool for ensuring robust control and stabilization across a wide array of dynamic systems.

Furthermore, SMC shines in its ability to effectively control and stabilize chaotic systems, characterized by their extreme sensitivity to initial conditions and inherently unpredictable nature [6]. Encountered in a wide range of disciplines such as physics [7], chemistry [8], image encryption [9], biology [10], and engineering [11], these systems exhibit complex, erratic, and seemingly random behaviors. Controlling such systems poses a significant challenge, particularly when conventional linear control strategies fall short.

The essence of Sliding Mode Control (SMC) lies in designing a control signal that propels the system onto a designated sliding surface, ultimately guiding it toward the desired state. This control mechanism ensures that the system’s trajectory swiftly converges and stays anchored to the sliding surface. Employing a distinct, discontinuous control strategy, SMC actively steers the system towards the surface, achieving rapid and sustained convergence. Once secured on the sliding surface, the control is fine-tuned to maintain the system’s trajectory there. This foundational approach exemplifies the inherent flexibility and precision of SMC, empowering meticulous manipulation of the system’s trajectory through deliberate control actions.

Choosing the right sliding surface is crucial to the success of Sliding-Mode Control (SMC). It needs to be designed specifically to achieve the desired control goal. For example, if the goal is to track a specific reference trajectory, the sliding surface should closely mirror that trajectory. This close alignment ensures that the control mechanism effectively steers the system’s behavior toward the desired outcome, highlighting the critical role of the sliding surface in achieving precise and targeted control.

In the classical stability assessment, the error defining the sliding surface usually reflects the difference between a system's current state and its intended equilibrium point. However, our focus on structural stability necessitates replacing the traditional tracking error with what we call the synchronization error. This error quantifies the deviation between the system's current state and its state delayed by one period of unstable periodic orbits (UPOs). This shift in perspective allows us to explore the system's resilience and its ability to synchronize its dynamics with a structurally stable desired trajectory.

To identify the characteristics of UPOs with precision, we employ the well-established Poincare section method ´ [12], [13]. This involves constructing a Poincare section ´ by intersecting the UPO with a carefully chosen plane in the phase space. The UPO's period is then determined by measuring the time between consecutive crossings of the UPO through this section.

To validate the closed-loop system's stability, we will leverage Lyapunov's theory. This approach will provide the necessary framework to confirm the system's stability under the implemented control strategies.

The remainder of this paper is structured as follows: Section II outlines the stabilization problem. Section III presents the control strategy development in two parts: Section III-A details its creation, and Section III-B showcases its effectiveness through computational simulations using the Rossler system as a benchmark, focusing on various unstable periodic orbits (UPOs). These simulations validate the theoretical concepts and demonstrate the effectiveness of the proposed method.

II. PROBLEM FORMULATION

This section delves into the challenge of controlling and stabilizing chaotic systems using Sliding Mode Control (SMC). We begin by introducing a benchmark chaotic system, described as follows:

$$x^n = f(x) + b(x)u \tag{1}$$

Where :

- $x \in R^n$ is the n-dimensional state vector.
- $u \in R^i$ is the i-dimensional control vector to be determined.
- n is the system order.
- i is the number of control inputs, with $i \leqslant n$.
- $f(x)$ and $b(x)$ are nonlinear functions with appropriate dimensions.

The basic idea of sliding mode control is to force the system to follow a predefined trajectory by constraining its dynamics to slide along a specific surface, known as the sliding surface. The sliding surface is designed to be a function of the state of the system and the predefined trajectory (desired trajectory). In our case, we choose the delayed states as the desired trajectory, where the delay time of the state corresponds to the time it takes for the system to complete one cycle of the target UPO. So, as described in [14], the sliding surface is given as:

$$S_i(t) = (\frac{d}{dt} + \lambda_i)^{n-1} e_i \tag{2}$$

The tracking error, denoted by e_i, is defined as the difference between the system's current state and its state delayed by a time τ, equal to the period of an Unstable Periodic Orbit (UPO). This error is represented as:

$$e_i = x_i(t) - x_i(t-\tau) \tag{3}$$

where:

- e_i: is the tracking error for the i^{th} state variable.
- $x_i(t)$: is the current value of the i^{th} state variable
- $x_i(t-\tau)$: is the value of the i^{th} state variable delayed by τ.
- τ: is the delay time equal to the UPO period.
- λ: Strictly positive constant.

For instance, if the system order is $n = 2$ n, the equation 2 become:

$$S_i(t) = \dot{e}_\iota + \lambda_i e_i \tag{4}$$

When the system operates in sliding mode, it satisfies the following conditions [15], [16]:

$$\begin{cases}\lim_{t\to\infty} S_i(t) = 0 \\ \lim_{t\to\infty} \dot{S}_i(t) = 0\end{cases} \quad (5)$$

Our objective is to design a control law that steers the tracking error (3) towards zero, essentially ensuring that the system's behavior closely follows the desired trajectory (delayed state). To achieve this, we leverage the sliding condition (5) as a critical tool, setting a specific requirement that guarantees the error diminishes over time. However, the system (1) satisfies the reachability criterion only if it meets the necessary and sufficient condition outlined by the Lyapunov theorem.

$$\begin{matrix}\frac{1}{2}\frac{d}{dt}(S^2) \leqslant 0 \\ \Rightarrow S^T\dot{S} \leqslant 0\end{matrix} \quad (6)$$

Where $S = [S_1\, S_2 \ldots S_n]^T$

The condition (6) ensures that the state trajectory of the system eventually reaches the sliding surface. This establishes a more stringent reachability criterion known as the "η-condition" [17].

$$\begin{matrix}S^T\dot{S} \leqslant -\eta|S| \\ \Rightarrow \dot{S} \leqslant\leqslant -\eta_i sgn(S_i)\end{matrix} \quad (7)$$

We replace the values of S from equation (4) in the equation (7) then we get:

$$\ddot{e}_i + \lambda_i \dot{e}_i \leqslant -\eta_i sgn(S_i) \quad (8)$$

Where sgn is the sign function and $\eta_i (i = 1, 2 \ldots n)$ are strictly positive constants.

To guarantee stability and effectively manage uncertainties and disturbances within the closed-loop system, we construct sliding-mode control laws, denoted by $u_{si} (i = 1, 2 \ldots n)$. These laws aim to steer the system's dynamics towards the sliding surfaces, defined by $(S(t) = 0)$. The specific formulation of these control laws is presented as follows:

$$u_{si} = -S_i - \eta_i sgn(S_i) \quad (9)$$

III. NUMERICAL EXAMPLE

The field of chaos theory provides a wealth of benchmark chaotic systems that function as standardized models for testing and validation in research. For this study, we have chosen the widely recognized Rössler system as our example. This system, first proposed by Otto Rössler in 1976 [18], is described by three nonlinear ordinary differential equations, presented as follows:

$$\begin{cases}\dot{x}(t) = -y(t) - z(t) \\ \dot{y}(t) = x(t) + ay(t) \\ \dot{z}(t) = b + z(t)(x(t) - c)\end{cases} \quad (10)$$

where x, y, and z are the state variables, and a, b, and c are constants. The values of these constants determine the behavior of the system.

The Rossler system exhibits chaotic behavior for certain parameter values, so for this aim, we choose the values of a, b, and c as $0.2, 0.2$ and 5.7, respectively. As a chaotic system, its trajectories are highly sensitive to initial conditions.

Figure 1 illustrates the dynamics of the Rössler system, resulting in blue and red trajectories, respectively, for the initial conditions of $[0.2, 0.2, 0.2]$ and $[0.25, 0.25, 0.25]$. Figure 2 further demonstrates the evolution of the state of the system over time.

Figures 1 and 2 demonstrate clearly the Rössler system's chaotic nature, highlighting its high sensitivity to minor changes in initial conditions or parameters. This sensitivity leads to significant changes in the system's behavior over time. In support of this, Wolf's algorithm [19] was used to calculate the Lyapunov exponents, resulting in $\lambda_1 = 0.070$, $\lambda_2 = 0.000$, and $\lambda_3 = -5.400$. The presence of a positive Lyapunov exponent (λ_1) unequivocally confirms the chaotic behavior of the Rössler system under these parameters.

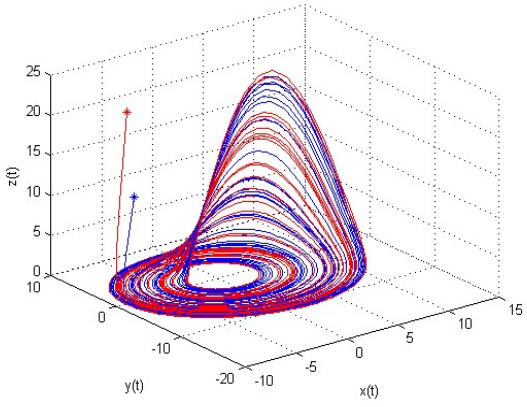

Fig. 1. Rossler System behavior for different initial conditions.

This finding highlights the need for a control strategy to instill structural stability in the system, guiding it towards more predictable and manageable dynamics.

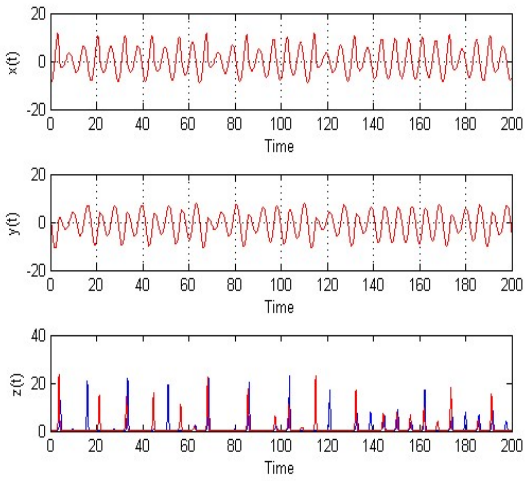

Fig. 2. Time behavior of $x(t), y(t)$ and $z(t)$ states without control.

IV. CONTROL LAW

The system 10 with the control law can be written as follows:

$$\begin{cases} \dot{x}(t) = -y\,(t) - z(t) + u_1 \\ \dot{y}(t) = x(t) + ay(t) + u_2 \\ \dot{z}(t) = b + z(t)(x(t) - c) + u_3 \end{cases} \tag{11}$$

The tracking error vector between the Rossler system's present state and its delayed state is given by :

$$\begin{cases} e_1(t) = x(t) - x(t-\tau) \\ e_2(t) = y(t) - y(t-\tau) \\ e_3(t) = z(t) - z(t-\tau) \end{cases} \tag{12}$$

Its time derivative can be expressed as:

$$\begin{cases} \dot{e}_1(t) = \dot{x}(t) - \dot{x}(t-\tau) \\ \dot{e}_2(t) = \dot{y}(t) - \dot{y}(t-\tau) \\ \dot{e}_3(t) = \dot{z}(t) - \dot{z}(t-\tau) \end{cases} \tag{13}$$

$$\Rightarrow \begin{cases} \dot{e}_1(t) = -e_2(t) - e_3(t) + u_1(t) \\ \dot{e}_2(t) = e_1(t) + ae_2(t) + u_2(t) \\ \dot{e}_3(t) = e_1(t)e_3(t) + z(t-\tau)e_1(t) + x(t-\tau)e_3(t) \\ \qquad -ce_3(t) + u_3(3) \end{cases} \tag{14}$$

Now we insert the values of e_i and $\dot{e}_i$ in the equation 4 to define the sliding surfaces as follows:

$$\begin{cases} s_1(t) = \dot{e_1}(t) + k_1 e_1(t) \\ s_2(t) = \dot{e_2}(t) + k_2 e_2(t) \\ s_3(t) = \dot{e_3}(t) + k_3 e_3(t) \end{cases} \tag{15}$$

where k_1, k_2 and k_3 are positive real numbers. Finally, the control law of equation 9 can be re-expressed as :

$$\begin{cases} u_1(t) = -ke_1 + e_2 + e_3 - \eta sgn(s_1) \\ u_2(t) = -k_2 e_2 - e_1 - ae_2 - \eta sgn(s_2) \\ u_3(t) = -k_3 e_3 - e_1 e_3 - z(t-\tau)e_1 - x(t-\tau)e_3 \\ \qquad +ce_3 - \eta sgn(s_3) \end{cases} \tag{16}$$

V. RESULTS

Continuing our analysis of the Rössler system, defined in equation (10), we start with arbitrary initial conditions of $[0.2, 0.2, 0.2]$ and parameter values of $[a, b, c] = [0.2, 0.2, 5.7]$. The proposed controller is activated at $t = 150$ seconds, using controller constants k_1, k_2, k_3 and η set to $60, 40, 400$ and 0.05, respectively.
For the initial simulation results shown in figures 3, 4, and 5, the time delay τ is chosen to match the first Unstable Periodic Orbit (UPO) cycle, specifically $\tau = T_1 = 5.88$. In subsequent simulations, shown in figures 6, 7, and 8, the time delay is adjusted to match the second UPO cycle, with $\tau = T_2 = 11.76$.

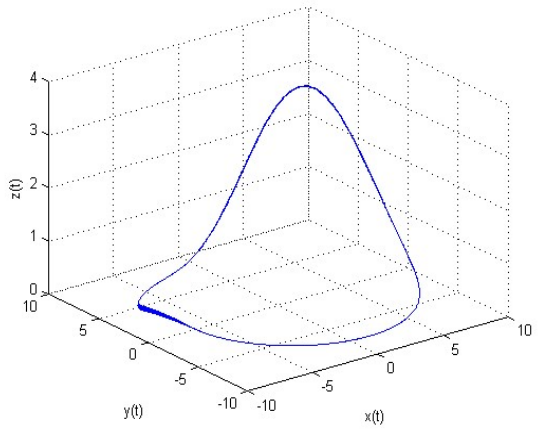

Fig. 3. Rossler System behavior with the control actions u_1, u_2 and u_3 and $\tau = T_1 = 5.88$.

Figure 3 illustrates the system exhibiting a behavior that is both singular and periodic, representing the most basic and predictable form of dynamic system response.

To further illustrate this point, Figure 4 delves into the system's behavior over time, both before and after activating the proposed controller. We observe a swift stabilization of the system within the initial cycle starting at $t = 150$ seconds, leading to a periodic behavior of the Rössler system. This shift towards predictability highlights the effectiveness of the proposed control strategy in stabilizing the system and facilitating more manageable and predictable dynamics.

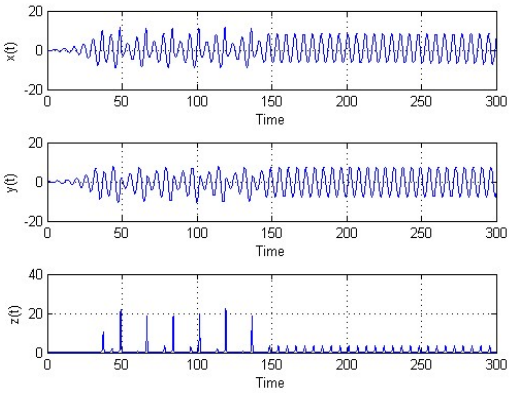

Fig. 4. Time response $x(t), y(t)$ and $z(t)$.

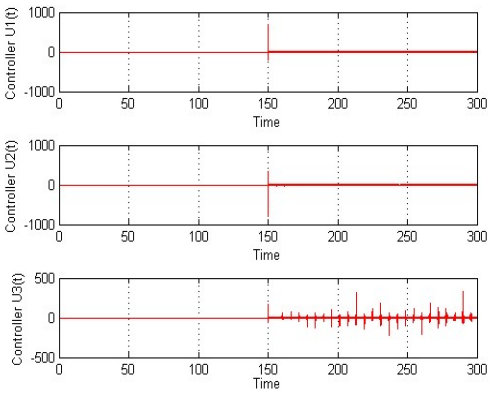

Fig. 5. Evolution of the control actions u_1, u_2 and u_3.

Figure 5 shows that after the stabilization process, the control signal is reduced to zero, allowing the Rössler system to maintain its stable period-one behavior. This highlights the controller's dual ability to both stabilize and maintain the predictability of chaotic systems effectively. Furthermore, the vanishing control signal indicates that continuous control input is not necessary for sustained stability. This attribute makes the proposed control method energy-efficient and practical, suggesting its potential for broader application in managing chaotic dynamics with minimal energy consumption.

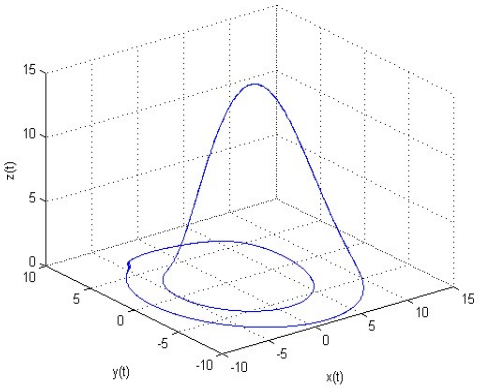

Fig. 6. Rossler System behavior with the control actions u_1, u_2 and u_3 and $\tau = T_2 = 11.76$.

Figure 6 shows that when the time delay matches the second period, the system exhibits a two-periodic behavior. Similarly to the first simulation, activating the controller at $t = 150$ seconds leads to the system stabilizing in the second period of the unstable periodic orbit (UPO), as seen in Figure 7. After stabilization, the control signal approaches zero, as illustrated in Figure 8. This behavior reinforces the controller's effectiveness in guiding the system towards stability and achieving a predictable pattern, all while minimizing ongoing control input, as evidenced by the diminishing control signal.

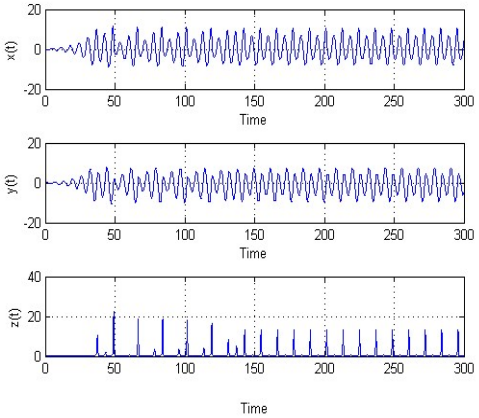

Fig. 7. Time response $x(t), y(t)$ and $z(t)$.

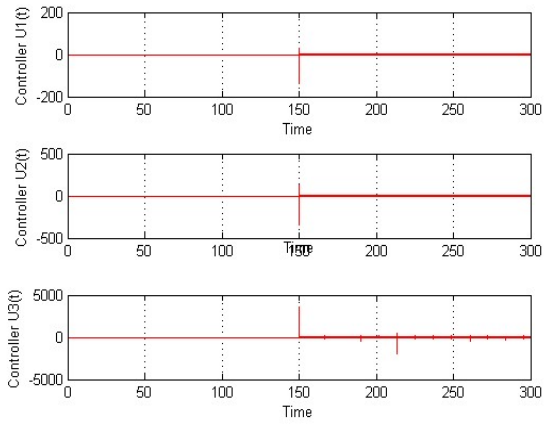

Fig. 8. Evolution of the control actions u_1, u_2 and u_3.

VI. CONCLUSION

This study introduces a novel sliding-mode control strategy to stabilize chaotic systems. Its key innovation lies in the selection of the tracking error for the sliding surfaces. Unlike traditional approaches, the tracking error incorporates the system's state delayed by one period of unstable periodic orbits (UPOs) as a reference point, refining the concept of tracking error. The widely recognized Rössler system, chosen for its universality, serves as a test case to validate the method's effectiveness. Grounded in Lyapunov stability theory, the technique offers significant flexibility in choosing control parameters, enabling precise stabilization of the Rössler system at one of its most predictable UPOs. Simulations demonstrate the method's effectiveness, highlighting its simplicity, speed, robustness, and precision in achieving structural stability across a wide range of chaotic systems.

VII. REFERENCES

[1] V. Utkin, “Variable structure systems with sliding modes,” IEEE Transactions on Automatic control, vol. 22, no. 2, pp. 212–222, 1977.

[2] X. Sun, L. Zhang, and J. Gu, “Neural-network based adaptive sliding mode control for takagi-sugeno fuzzy systems,” Information Sciences, vol. 628, pp. 240–253, 2023.

[3] M. Waseem and I. Ali, “Tracking error control of robotic manipulator using optimal integral sliding mode control in the presence of external disturbances,” in 2023 4th International Conference on Computing, Mathematics and Engineering Technologies (iCoMET). IEEE, 2023, pp. 1–6.

[4] S. Kode, Y. Shtessel, A. Levant, J. Rakoczy, M. Hannan, and J. Orr, “Development of relative degree based aerospace sliding mode control matlab toolbox with case studies,” IEEE Aerospace and Electronic Systems Magazine, 2022.

[5] S. Zeghlache, M. Z. Ghellab, A. Djerioui, B. Bouderah, and M. F. Benkhoris, “Adaptive fuzzy fast terminal sliding mode control for inverted pendulum-cart system with actuator faults,” Mathematics and Computers in Simulation, 2023.

[6] H. G. Schuster and W. Just, Deterministic chaos: an introduction. John Wiley & Sons, 2006.

[7] H. Jahanshahi, O. Orozco-Lopez, J. M. Munoz-Pacheco, N. D. Alotaibi, ´ C. Volos, Z. Wang, R. Sevilla-Escoboza, and Y. M. Chu, “Simulation and experimental validation of a non-equilibrium chaotic system,” Chaos, Solitons & Fractals, vol. 143, p. 110539, 2021.

[8] A. Adechinan, Y. Kpomahou, L. Hinvi, and C. Miwadinou, “Chaos, co- ´ existing attractors and chaos control in a nonlinear dissipative chemical oscillator,” Chinese Journal of Physics, vol. 77, pp. 2684–2697, 2022.

[9] R. Anandkumar, K. Dinesh, A. J. Obaid, P. Malik, R. Sharma, A. Dumka, R. Singh, and S. Khatak, “Securing e-health application of cloud computing using hyperchaotic image encryption framework,” Computers and Electrical Engineering, vol. 100, p. 107860, 2022.

[10] Y. Zhang, H. Xie, J. Sun, and H. Zhang, “An efficient multi-level encryption scheme for stereoscopic medical images based on coupled chaotic system and otsu threshold segmentation,” Computers in Biology and Medicine, vol. 146, p. 105542, 2022.

[11] B. Liang, C. Hu, Z. Tian, Q. Wang, and C. Jian, “A 3d chaotic system with multi-transient behavior and its application in image encryption,” Physica A: Statistical Mechanics and its Applications, p. 128624, 2023.

[12] Y. G. Zheng and M. H. Liu, “Stabilizing unstable periodic orbits in large stability domains with dynamic time-delayed feedback control,” Journal of the Franklin Institute, vol. 359, no. 16, pp. 8484–8496, 2022.

[13] D. Liu and H. Yamaura, “Stabilization control for giant swing motions of 3-link horizontal bar gymnastic robot using multiple-prediction delayed feedback control with a periodic gain,” Journal of System Design and Dynamics, vol. 5, no. 1, pp. 42–54, 2011.

[14] J. E. Slotine, W. Li et al., Applied nonlinear control. Prentice hall Englewood Cliffs, NJ, 1991, vol. 199, no. 1.

[15] S. Vaidyanathan and C.-H. Lien, Applications of sliding mode control in science and engineering. Berlin (Germany): Springer, 2017, vol. 709.

[16] V. I. Utkin, “Sliding modes and their applications in variable structure systems,” Mir, Moscow, 1978.

[17] J. Liu, Y. Gao, Y. Yin, J. Wang, W. Luo, and G. Sun, Sliding mode control methodology in the applications of industrial power systems. Springer, 2020.

[18] [18] V. Rybin, A. Tutueva, T. Karimov, G. Kolev, D. Butusov, and E. Rodionova, "Optimizing the synchronization parameters in adaptive models of rossler system," in ¨ 2021 10th Mediterranean Conference on Embedded Computing (MECO). IEEE, 2021, pp. 1–4.

[19] A. Wolf, J. B. Swift, H. L. Swinney, and J. A. Vastano, "Determining lyapunov exponents from a time series," Physica D: nonlinear phenomena, vol. 16, no. 3, pp. 285–317, 198.